Syracuse University

SURFACE

Physics

College of Arts and Sciences

Monte Carlo Renormalization of 2d Simplicial Quantum Gravity Coupled to Gaussian Matter

Simon Catterall
Syracuse University

Eric B. Gregory
Syracuse University

G. Thorleifsson
Facult¨at f¨ur Physik, Universit¨at Bielefeld D-33615, Bielefeld, Germany

Follow this and additional works at: https://surface.syr.edu/phy

Part of the Physics Commons

Recommended Citation

Monte Carlo Renormalization of 2d Simplicial Quantum Gravity Coupled to Gaussian Matter

E.B. Gregory [a], *S.M. Catterall* [a] and *G. Thorleifsson* [b]

[a] Physics Department, Syracuse University, Syracuse, NY 132144, USA
[b] Facultät für Physik, Universität Bielefeld D-33615, Bielefeld, Germany

Abstract

We extend a recently proposed real-space renormalization group scheme for dynamical triangulations to situations where the lattice is coupled to continuous scalar fields. Using Monte Carlo simulations in combination with a linear, stochastic blocking scheme for the scalar fields we are able to determine the leading eigenvalues of the stability matrix with good accuracy both for $c_M = 1$ and $c_M = 10$ theories.

1 Introduction

Dynamical triangulations offer a powerful way to investigate two-dimensional quantum gravity and, when coupled to scalar fields, bosonic string theories. This manner of discretizing such theories allows the use of techniques drawn from statistical mechanics. Great strides have been made in analytically understanding such models, notably with the development of matrix model techniques for solving the discrete systems and continuum approaches based on quantizing Liouville theory [1]. However, all these analytic approaches break down when applied to systems whose matter central charge c_M is greater than unity. Furthermore, the analytic approaches allow us to compute only correlation functions of *integrated* operators — they yield very little information on the nature of the quantum geometry or physically interesting questions concerning matter field correlators defined on geodesic paths.

To answer such questions, we must rely on Monte Carlo simulation techniques. Combining this powerful numerical tool with another, the renormalization group, in the form of the Monte Carlo Renormalization Group (MCRG), provides new insight into the critical behavior and hence the continuum limit for these models.

In this paper we describe our efforts to develop an efficient and functional blocking scheme for models of continuous scalar fields coupled to 2d dynamical triangulations.

We first introduce the class of model we consider and describe our simulation algorithm. Then we discuss real-space renormalization groups (RG) and the particular blocking schemes we have investigated. The primary goal of this work has been to extend the MCRG techniques, developed in Ref. [2], to continuous scalar fields. As a test of this method we have investigated models of one ($c_M = 1$) and ten ($c_M = 10$) scalar fields coupled to two-dimensional gravity respectively. The former model is chosen as it is solvable in the continuum, the latter as it represents a system where the back-reaction of matter is so strong that the internal geometry degenerates into polymer-like structure. As this RG method involves blocking a dynamical geometry, we start by demonstrating that it preserves the relevant fractal structure of the triangulations, characterized by such geometric exponents as the Hausdorff dimension d_H and the string susceptibility exponent γ_s. For the matter sector we have applied a linear stochastic blocking scheme to the fields and, for both the models we consider, after optimizing the blocking procedure, we determine the critical exponents governing the rescaling of the fields.

2   Model and Numerical Approach

The model we examine is a two-dimensional dynamically triangulated surface coupled to D copies of Gaussian scalar fields. It has a canonical (fixed area) partition function

$$Z = \sum_{\tau, \phi} e^{-S_\tau[\phi]}, \tag{1}$$

where the sum is over all possible combinatorial triangulations[1] τ, as well as over all possible configurations of the fields ϕ. The action,

$$S[\phi] = \sum_{\mu=1}^{D} \sum_{<i,j>} \left(\phi_i^\mu - \phi_j^\mu \right)^2, \tag{2}$$

depends on $\mu = 1, ..., D \;\; (= c_M)$ scalar fields ϕ^μ, and the second sum is over all nearest neighbor lattice points, i and j. Notice that due to the back-reaction of the matter fields on the geometry, coupling multiple copies of scalar fields to dynamical triangulations leads to genuinely different statistical systems, as the partition functions do not factorize, in contrast to the behavior on a regular lattice. In this paper we investigate models with one and ten fields, corresponding to matter with central charge $c_M = 1$ and 10 respectively.

The partition function Eq. (1) is evaluated numerical using Monte Carlo methods. The triangulations are update using a standard link-flip move — a link l_{ab} connecting two adjacent triangles t_{abc} and t_{bad} is removed and replaced by the link l_{cd}. We accept or reject such a move based on a Metropolis test.

---

[1] A priori, different ensembles of triangulations can be used provided they lead to a well defined partition function Eq. (1). In this work we use combinatorial triangulations, excluding self-energy and tadpole diagrams from the corresponding dual graph, as this simplifies the geometric blocking.
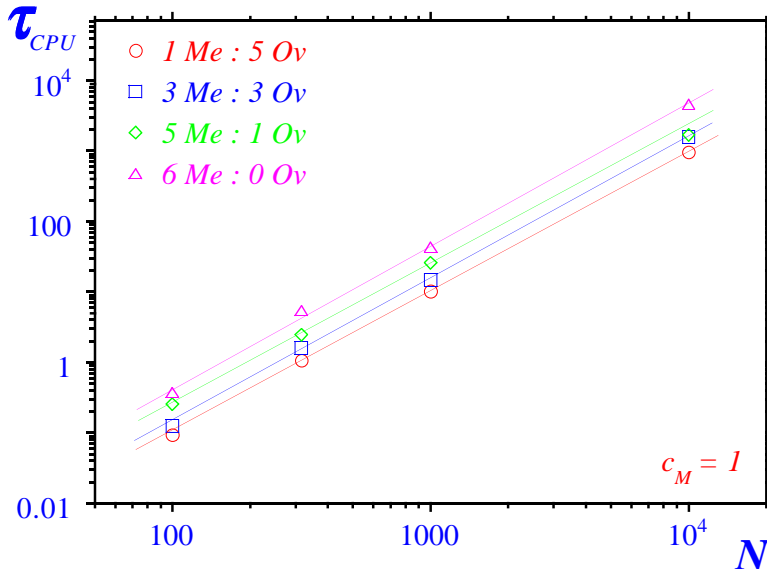
Figure 1: The auto-correlation time τ_{CPU}, measured in real-time, for different volumes N and for different ratios of Metropolis *versus* overrelaxation updates. The auto-correlations are estimated for the slowest mode, the radius of gyration $\sum_i \phi_i^2$, for the model Eq. (1) coupled to one scale field.

Updates of the Gaussian fields proceed in two ways. The first is a standard Metropolis update, where a small (local) change in the fields is accepted/rejected based on a Metropolis test. However, as this updating procedure suffers from very long auto-correlations we also employ an overrelaxation algorithm to update the fields. This involves replacing one of the fields at a node i with

$$\phi_i \ \to \ \phi_i' \ = \ \left[\frac{2}{q_i} \sum_{<i,j>} \phi_j \right] - \phi_i \ , \tag{3}$$

where j indexes the q_i neighbors of i. Since $\sum_{<i,j>}(\phi_i - \phi_j)^2 = \sum_{<i,j>}(\phi_i' - \phi_j)^2$, the action is preserved and the move is automatically accepted. The overrelaxation algorithm is, however, non-ergodic and some amount of Metropolis updates have to be included. We find, nonetheless, that by using a ratio of only one Metropolis update to every five overrelaxation updates the auto-correlations, measured in real-time, are reduced by about a factor of four compared to a pure Metropolis update. This is illustrated in Figure 1. This reduction can be understood qualitatively as the overrelaxation suppresses the usual random walk behavior of local updating algorithms [3]. However, in contrast to overrelaxation applied to scalar fields on a regular lattice [4], on dynamical triangulations critical slowing down is not reduced, only the overall prefactor — the dynamics of the updating procedure are dominated by the local geometric moves.

3

3   Monte Carlo Renormalization

A powerful tool for investigating the critical behavior of statistical systems is the renormalization group. The usual approach is to use some "course graining" procedure whereby the system is blocked or replaced by one with fewer degrees of freedom, effectively integrating out the short distance fluctuations while preserving the long-distance physics of the system. This renormalization group operation can be written in terms of a projection operator, $\mathcal{P}$, that maps the system from the old degrees of freedom to the new ones while preserving the partition function Eq. (1):

$$\mathrm{e}^{\,S'[\phi']} \; = \; \sum_\phi \mathcal{P}\left[\phi',\phi\right]\mathrm{e}^{S[\phi]}, \qquad \text{with} \qquad \sum_{\phi'} \mathcal{P}\left[\phi',\phi\right] \; = \; 1. \tag{4}$$

In general, upon application of the renormalization group the action $S[\phi]$, expanded on a suitable basis of operators $\{\mathcal{O}_\alpha\}$, changes according to

$$S \; = \; \sum_\alpha K_\alpha \mathcal{O}_\alpha \; \xrightarrow{\mathcal{P}} \; S' \; = \; \sum_\alpha K'_\alpha \mathcal{O}'_\alpha. \tag{5}$$

The K's and the $\mathcal{O}$'s are coupling constants and operators defined on the bare lattice, while their primed counterparts denote the corresponding quantities on the blocked lattice. Repeated iteration of the RG transformation leads to a flow in the associated coupling constants towards a fixed point $\{K^*\}$:

$$\{K\}^{(0)} \; \xrightarrow{\mathcal{P}} \; \{K\}^{(1)} \; \xrightarrow{\mathcal{P}} \; ... \; \xrightarrow{P} \; \{K^*\}. \tag{6}$$

A linearized approximation to the RG transformation in the vicinity of a critical (unstable) fixed point:

$$\delta K_\alpha^{(k+1)} \; = \; K_\alpha^{(k+1)} - K_\alpha^* \; \simeq \; \sum_\beta \left.\frac{\partial K_\alpha^{(k+1)}}{\partial K_\beta^{(k)}}\right|_{\mathbf{K}=\mathbf{K}^*} \delta K_\beta \; \equiv \; \sum_\beta T_{\alpha\beta}\, \delta K_\beta^{(k)}, \tag{7}$$

yields an eigenvalue equation for the stability matrix $T_{\alpha\beta}$,

$$\sum_\beta T_{\alpha\beta}\, u_\beta^i \; = \; \lambda_i\, u_\alpha^i. \tag{8}$$

An eigenvalue λ_i, corresponding to a relevant operator u_α^i in the effective action, defines a critical exponent y_i associated with the fixed point: $\lambda_i \; = \; b^{y_i}$, where $b = N^{(k)}/N^{(k+1)}$ is the volume blocking factor.

For some simple systems one may be able to write down an exact expression for the projection operator $\mathcal{P}$ and determine the critical properties explicitly from the stability matrix. In general, though, this is not possible. For dynamical triangulations, where the blocking involves both the geometry and the fields living on the surface, this task is even more complicated. Especially since, as discussed in next section, an explicit form of a projection operator for blocking the geometry is not available. For these reason we resort to a Monte Carlo Renormalization Group
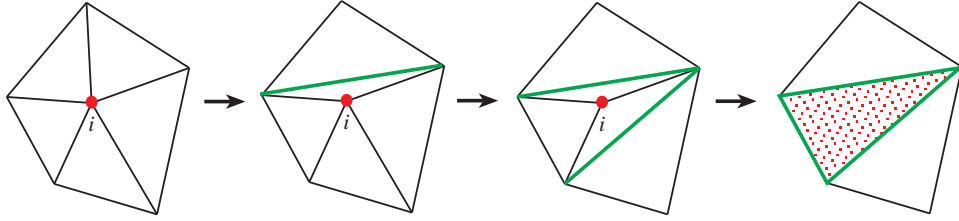
Figure 2: Node decimation: A sequence of link-flips around the selected node i reduce its coordination number to three. Then the node is removed, leaving a new triangle in its place.

procedure. This allows the determination of the elements of the stability matrix through Monte Carlo simulations in combination with a local blocking method for both the fields and the geometry:

$$\frac{\partial \langle \mathcal{O}_\gamma^{(k+1)} \rangle}{\partial K_\alpha^{(k)}} = \sum_\alpha \frac{\partial K_\alpha^{(k+1)}}{\partial K_\beta^{(k)}} \frac{\partial \langle \mathcal{O}_\gamma^{(k+1)} \rangle}{\partial K_\alpha^{(k+1)}} , \qquad (9)$$

where

$$\frac{\partial \langle \mathcal{O}_\gamma^{(k')} \rangle}{\partial K_\alpha^{(k)}} = \langle \mathcal{O}_\gamma^{(k')} \rangle \langle \mathcal{O}_\alpha^{(k)} \rangle - \langle \mathcal{O}_\gamma^{(k')} \mathcal{O}_\alpha^{(k)} \rangle . \qquad (10)$$

3.1 *Blocking the Geometry*

In dealing with fields on a dynamical triangulation we need a renormalization group prescription that integrates out the small scale feature of both the geometry and of the field configuration while preserving the large scale physics. The prescription we apply separates these two tasks. We first block the geometry independently from the fields by removing nodes at random, then assign new blocked scalar fields to the renormalized lattice. In this way the blocked triangulation serves as an inert scaffold for the field blocking. This method has previously been applied to an Ising model coupled to dynamical triangulations, where it yielded surprisingly accurate estimate of the critical properties of the model [2].

The general idea for blocking the lattice geometry utilizes a scheme called *node decimation*. This proceeds by randomly picking nodes and removing them from the triangulation. Removing a node with a coordination number q will leave a q–sided hole; that hole must be randomly triangulated. In practice, this is done by randomly flipping links around the selected node until its coordination number is reduced to three. Now when the node is removed the three-sided hole in the triangulation can be replaced by a triangle. This is illustrated in Figure 2. This procedure is then repeated until a fraction of the nodes, corresponding to a desired blocking factor b, has been removed.

The link-flips in the intermediate step are performed independent of the scalar fields residing on the adjacent nodes. This amounts to choosing the different re-triangulations of the polygonal hole with equal probability provided no geometric constraint is violated — demanding that the result is a combinatorial triangulations

may restrict the possible re-triangulations. As this restriction is non-local, it is not possible to write down an explicit projection operator for the node decimation. Alternative weight distributions for the re-triangulations where explored in Ref. [2]; however, the observed critical behavior was not very sensitive to the particular choice.

This blocking method is justified *a posteriori* by verifying that it preserves the long distance physics, or the fractal structure, of the geometry. This we do in Section 4.1.

3.2   *Blocking the Scalar Fields*

For the scalar fields we have applied a *linear* RG transformation to assign the block lattice fields. For a node i that survives the decimation procedure a new scalar field ϕ_i' is constructed as a function of the original fields ϕ on the bare lattice:

$$\phi_i' \;=\; \xi \left[\alpha \phi_i + (1-\alpha) \frac{1}{q_i} \sum_{j=1}^{q_i} \phi_j \right] + \frac{\chi}{\sqrt{a_w}} \,. \tag{11}$$

Here ξ is an overall rescaling of the fields, and α determines the relative weight between the contribution of field on the bare lattice node i and the contribution from its bare lattice neighbors ϕ_j. Notice that blocking is *stochastic* — χ is a Gaussian random noise with $\langle \chi^2 \rangle = 1$. The amplitude of the noise depends on a auxiliary parameter a_w.

The RG transformation Eq. (11) can be expressed in terms of a projection operator

$$\mathcal{P}\left[\phi',\phi\right] \;=\; \exp \left[-\frac{a_w}{2} \sum_i \left(\phi_i' - \xi \left[\alpha \phi_i + (1-\alpha) \frac{1}{q_i} \sum_{j=1}^{q_i} \phi_j \right] \right)^2 \right], \tag{12}$$

and depends on *three* parameters: α, ξ and a_w. As these parameters are crucial for a successful blocking procedure it is necessary to establish some criteria for how to choose their optimal values:

(i)   The relative weight α, between the contribution from the fields on the initial bare lattice node and on its neighboring nodes, must be chosen appropriate for the particular geometric blocking factor $b = N'/N$ being used. Clearly as $b \to 1$, α should approach one, and as b grows α should decrease. However, we have found that in practice this scheme is fairly robust under reasonable choices of α. In this paper we us $\alpha = 0.5$.

(ii)   The amount of noise in the blocking procedure is controlled by the parameter a_w. In general each choice of a_w will lead, under renormalization, to a local fixed point. This results in a line of fixed points, all corresponding to the same continuum limit but differing in the range of their interactions on the lattice. For an optimal RG transformation the value of a_w should correspond to as local effective action as possible and, in addition, should bring us in a vicinity of a fixed point with a

minimal amount of blocking. In practice, the optimal value a_w^* is determined as the one yielding the most rapid convergence of the eigenvalues λ_i in the blocking procedure.

(**iii**) The most difficult is the determination of an appropriate value for ξ — the *field renormalization constant*. In general, an arbitrary choice of ξ will produce fixed point behavior, but only with one choice, ξ^* will the action flow towards the non-trivial, local fixed point representing the continuum limit. Therefore simply looking for stability of eigenvalues is not sufficient to determine ξ^*. One option is to keep the expectation value of some long-range observable, such as the radius of gyration $\langle \phi^2 \rangle$, fixed under the blocking (as done by Lang [5]). We use, however, an alternative method discussed in Ref. [6]. It uses the property of the theory Eq. (1) that an arbitrary re-scaling of the fields does not change the physical content. This implies that the fixed point action should include a marginal operator corresponding to these (redundant) perturbations. Associated to the marginal operator is a sub-leading eigenvalue equal to one; requiring that such an eigenvalue exist in the spectrum of the stability matrix provides a criteria for choosing the optimal value ξ^*.

To summarize our strategy: We determine a_w^* as the value yielding the most stable eigenvalues of the stability matrix. Using this value of a_w, we then determine the correct renormalization constant ξ^* by looking for a marginal sub-leading eigenvalue.

In calculating the stability matrix in the MCRG analysis, we have used the following basis of field operators:

$$\mathcal{O}_m \;=\; \sum_i \phi_i \Box^m \phi_i \,, \qquad m = 0, 1, 2... \,, \tag{13}$$

where

$$\Box \phi_i \;=\; \sum_{\langle ij \rangle} \phi_j - q_i \phi_i \,. \tag{14}$$

Measured in lattice units, an operator $\phi_i \Box^m \phi_i$ extends m steps away from the node i. Hypothetically, a lattice of volume N could require a basis with operators up to order $m \sim N^{1/d_H}$; in practice, however, including operators with $m \le 4$ proved to be sufficient.

4   Numerical Results

We have simulated the model Eq. (1) for one and ten scalar fields on triangulations of up to $N = 4000$ triangles. A typical run consisted of about five million sweeps, each sweep includes approximately N link-flips, N Metropolis updates, and $10N$ overrelaxation updates. For each volume we collected and stored few thousand independent configurations, each of which is then blocked using a node decimation with a volume blocking factor $b = 2$. Storing the configurations was essential as it allowed us to repeat the blocking and to analyze a wide range of values of the parameters a_w and ξ.

Table 1: The fractal dimensions d_H, for ten scalar fields coupled to dynamical triangulations, after $k = 0$, 1, and 2 node decimations.

k	d_H
0	2.36(9)
1	2.29(7)
2	2.28(7)

4.1 *Geometric Properties*

To demonstrate that the node decimation preserves the long distance fractal structure of the geometry, we have measured two different geometric exponents: the internal *Hausdorff* or *fractal dimension d_H* and the *string susceptibility exponent γ_s*.

The Hausdorff dimension provides a measure of the intrinsic "dimensionality" of the triangulations and is defined by the volume of a geodesic ball with radius r: $v(r) \sim r^{d_H}$. A convenient way of measuring d_H in numerical simulations is provided by the node-node distribution function $n(r, N)$ — the number of nodes at a geodesic distance r from a marked node. Simple scaling arguments [7, 8] imply that

$$n(r, N) \;=\; N^{1-1/d_H} f\left(\frac{r}{N^{1/d_H}}\right), \tag{15}$$

and d_H is determined as the value that optimally "collapses" distributions $n(r, N)$, measured on different lattice volumes, on a single scaling curve. Notice, however, that in determining d_H on blocked triangulations only distributions $n^{(k)}(r, N)$ corresponding to the same amount of node decimation k should be included in the analysis.

In Table 1 we show the measured values of the fractal dimensions for $D = 10$ and node decimation $k = 0$, 1, and 2. For ten scalar fields coupled to dynamical triangulations, the geometry is expected to degenerate into branched polymers with $d_H = 2$. This is in reasonable agreement with what we observe, $d_H \approx 2.3$, especially as we use triangulations of relatively modest size[2]. The important observation is that the estimate of d_H does not change notably as the node decimation is iterated.

The string susceptibility exponent γ_s defines the leading singular behavior of the grand-canonical partition function: $Z(\mu) \approx Z_{\text{reg}} + (\mu - \mu_c)^{2-\gamma_s}$. This in turn implies that the canonical partition function behaves asymptotically as: $Z(N) \sim \exp(\mu_c N) \, N^{\gamma_s - 3}$. A powerful method to measure γ_s is provided by the distribution of *minimal neck baby universes* — a part of the triangulation connected to the rest *via* a minimal neck consisting of three links. The distribution of baby universes of size B on a triangulation of total volume N can be written as [10]:

$$b_N(B) \;\approx\; \frac{B\,Z(B)\,(N-B)\,Z(N-B)}{Z(N)} \;\sim\; (N-B)^{\gamma_s - 2} B^{\gamma_s - 2}. \tag{16}$$

---

[2]The Hausdorff dimension usually requires much larger triangulations for its accurate determination, especially if its value is large. This prevented us from measuring d_H for a single scalar field, where numerical simulations indicate $d_H \approx 4$ [9].
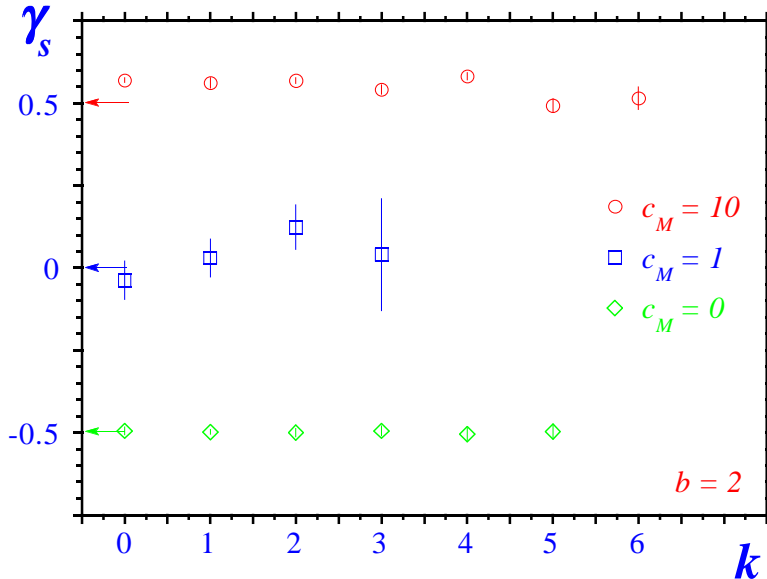
Figure 3: Measured values of the string susceptibility exponent γ_s *versus* the number of node decimations k, for zero, one and ten scalar fields coupled to $2d$–gravity.

By measuring the distribution $b_N(B)$ on a fixed volume, γ_s is determined by a fit to Eq. (16) [11].

We measured γ_s for $D = 0$, 1, and 10, and for up to six iterations of the node decimation[3]. The result is shown in Figure 3. And, just as for the fractal dimension, the values of γ_s proved to be remarkable stable as the blocking procedure is iterated, in some cases even after as much as 98% of the triangulation has been removed ($k = 6$). Combined, the measurements of d_H and γ_s provide strong evidence that the fractal structure is indeed preserved under this blocking scheme for both the models we consider.

4.2 *Stability Matrix for the Matter Sector*

We now turn to the blocking of the matter fields following the prescription in Section 3.2. We calculate the stability matrix $T_{\alpha\beta}(\phi, \phi')$ using the basis of operators Eq. (13). In principle, on a finite lattice operators of order $m \lesssim N^{1/d_H}$ could be included in the analysis; in practice, though, working with a large basis of operators is troublesome as it frequently leads to the appearance of complex (unphysical) eigenvalues. This necessitates a truncation of the basis; we found that including four operators provided sufficient overlap with the relevant operators in the fixed point action. We use a bare lattice of volume $N^{(0)} = 4000$, and a sequence of blocked lattices: $N^{(k)} = 2000$, 1000, 500, and 250, produced by $k = 1, 2, 3$, and, 4 node decimations, respectively. The field blocking was repeated several times using different

---

[3]For one scalar field the determination of γ_s is complicated by logarithmic corrections to the free energy Eq. (1). This requires a fit to a more complicated functional form than Eq. (16), which in turn reduces the precision with which γ_s is determined [11].

Table 2: The two largest eigenvalues of the stability matrix, λ_1 and λ_2, for one scalar field ($c_M = 1$), for different values of the parameter a_w, after up to four RG iterations k. A field renormaliztion $\xi = 1.00$ and basis of four field operators $\mathcal{O}_m$ is used in calculating $T_{\alpha\beta}$.

a_w	λ_1				λ_2			
	$k=1$	$k=2$	$k=3$	$k=4$	$k=1$	$k=2$	$k=3$	$k=4$
4	1.976(6)	1.961(16)	1.944(13)	1.927(25)	0.11(1)	0.24(5)	0.39(5)	0.40(4)
10	1.991(8)	2.002(10)	1.964(13)	1.987(19)	0.38(2)	0.49(4)	0.55(3)	0.55(4)
24	1.991(7)	1.994(8)	2.016(10)	1.980(16)	0.70(2)	0.78(3)	0.80(3)	0.81(2)
32	2.001(5)	1.991(9)	1.995(8)	2.001(12)	0.81(3)	0.81(3)	0.83(3)	0.83(3)
70	1.992(5)	1.988(8)	1.971(13)	1.974(15)	0.91(5)	0.97(3)	0.94(3)	1.02(3)
100	1.995(6)	2.001(8)	1.980(8)	1.975(14)	0.94(4)	1.02(3)	1.00(3)	1.00(2)
130	1.992(6)	1.998(5)	1.991(10)	1.980(19)	0.97(5)	0.99(4)	1.02(3)	1.00(2)
200	1.992(5)	1.992(7)	2.005(8)	1.997(16)	1.01(4)	1.04(3)	1.02(3)	1.03(3)
400	1.998(7)	1.984(9)	2.002(9)	1.973(11)	0.99(4)	1.04(3)	1.04(2)	1.07(3)
1000	1.992(5)	2.002(6)	1.976(8)	1.964(20)	1.05(4)	1.02(3)	1.00(3)	1.05(3)
10000	1.986(5)	1.999(8)	1.998(8)	1.991(15)	1.03(5)	1.02(4)	1.08(3)	1.02(2)
40000	1.990(5)	1.999(6)	2.001(9)	1.989(15)	0.99(7)	0.98(5)	1.04(4)	1.05(3)

sets of parameters, a_w and ξ, to determine their optimal values.

The simulations of one scalar field, $c_M = 1$, served as somewhat of a test case as analytical results are available. We found the leading and sub-leading eigenvalues, λ_1 and λ_2, to be remarkably insensitive to the choice of a_w, as long as $a_w > 50$. This is demonstrated in Table 2. This lower limit is understandable as for values of $a_w < 50$ the noise term in Eq. (11) becomes comparable in magnitude to the fields themselves. It is, on the other hand, rather surprising that suppressing the noise altogether, choosing $a_w \gg 50$, yields equally stable eigenvalues. Naively, one expects that a fully deterministic blocking, $a_w = \infty$, should lead to a less local fixed point action [6]. However, contrary to blocking scalar fields on a regular lattice, the randomness in blocking the geometry may introduce sufficient noise to limit the range of the interactions in the fixed point action.

The two leading eigenvalues do, on the other hand, depend strongly on the field renormalization constant ξ. This we show in Table 3 for different values of ξ and using, as a reasonable amount of noise, $a_w = 100$. Using the criteria that there should exist a (stable) marginal sub-leading eigenvalue, λ_2, we judge the optimal value to be $\xi^* = 1.00(3)$. The quoted error indicates the interval where λ_2 differs from unity by one standard deviations.

The combination, $\xi^* = 1$ and $a_w^* = 100$, yields a leading eigenvalue $\lambda_1 = 1.980(8)(90)(10)$. The numbers in the parentheses give the statistical error on λ_1, and the errors due to the uncertainty in ξ and a_w, respectively. The stability of the two leading eigenvalues under repeated RG iterations is shown in Figure 4.

We studied the model with ten scalar fields using the same procedure. The stability under blocking of the leading and sub-leading eigenvalues is shown for different amount of noise a_w in Table 4. We select the value $a_w = 100$ as the most optimal, though again, values of $a_w > 100$ all seem to produce relatively stable eigenvalues. In contrast to the $c_M = 1$ model, however, for $c_M = 10$ even
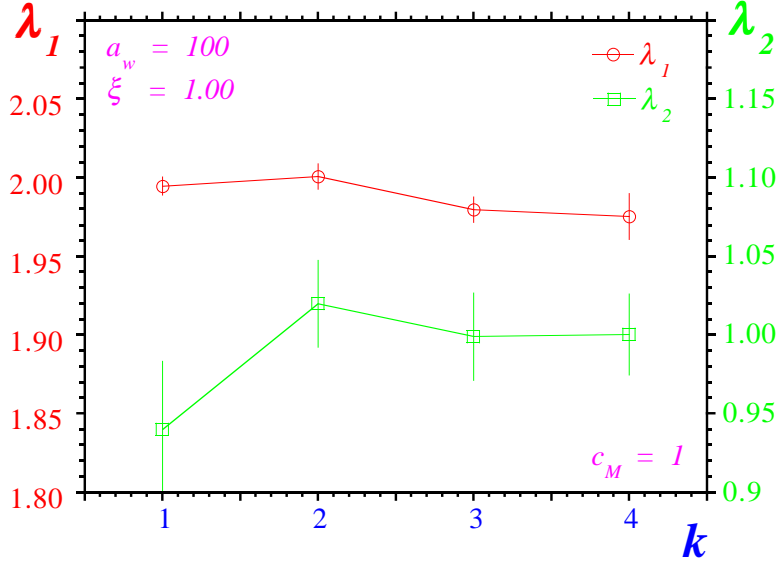
Figure 4: The two leading eigenvalues of the stability matrix for one scalar field ($c_M = 1$), calculated using $a_w = 100$ and $\xi = 1.00$, *versus* the number of RG iterations k.

Table 3: Same as in Table 2, except for varying field renormalization ξ but fixed amount of noise $a_w = 100$.

	λ_1				λ_2			
ξ	$k = 1$	$k = 2$	$k = 3$	$k = 4$	$k = 1$	$k = 2$	$k = 3$	$k = 4$
0.92	2.360(8)	2.350(10)	2.361(10)	2.340(22)	1.09(6)	1.14(4)	1.14(3)	1.11(4)
0.96	2.175(6)	2.166(10)	2.156(10)	2.148(20)	0.94(6)	1.09(4)	1.07(2)	1.08(2)
0.98	2.085(6)	2.076(6)	2.078(13)	2.064(18)	0.97(5)	1.06(3)	1.01(2)	1.04(3)
1.00	1.995(6)	2.001(8)	1.980(8)	1.975(14)	0.94(4)	1.02(3)	1.00(3)	1.00(2)
1.02	1.925(8)	1.907(6)	1.900(7)	1.903(13)	0.87(5)	1.00(4)	0.97(3)	0.99(2)
1.04	1.855(6)	1.848(4)	1.845(10)	1.837(13)	0.89(4)	0.93(3)	0.94(1)	0.95(2)
1.08	1.715(4)	1.705(5)	1.710 (8)	1.700(9)	0.84(4)	0.90(3)	0.89(2)	0.86(3)

using a bases of only four field operators leads occasionally complex and unphysical eigenvalues. This appears usually in the first iteration of the field blocking and for the sub-leading eigenvalue λ_2. We took this as indicating that the bare system is not sufficiently close to the critical fixed point for the linear approximation Eq. (7) to be valid; this observation is supported by the large change in the eigenvalues in the first iteration. This is not terribly troubling, though, as one can choose a_w such that in the successive blocking all of the eigenvalues are real.

In Table 5 we show the variation in the eigenvalues with the field renormalization. Using the same analysis as we did for $c_M = 1$, we find that $\xi = 0.92(4)$ gives a sub-leading eigenvalue close to unity for $c_M = 10$. This value, combined with $a_w = 100$, corresponds to a leading eigenvalue $\lambda_1 = 2.36(20)$. Here we just quote the dominant error due to the uncertainty in determining ξ^*. In Figure 5 we show the stability of the two largest eigenvalues as the fields are blocked using $\xi^* = 0.92$ and $a_w^* = 100$.

Table 4: Same as in Table 2, except for ten scalar fields, $c_M = 10$, and a different field renormalization, $\xi = 0.92$. The asterisk indicates a complex eigenvalue.

	λ_1				λ_2			
a_w	$k=1$	$k=2$	$k=3$	$k=4$	$k=1$	$k=2$	$k=3$	$k=4$
4	2.361(4)	2.339(8)	2.323(17)	2.290(21)	0.041(12)	1.27(11)	1.12(11)	1.07(14)
24	2.366(3)	2.360(6)	2.345(7)	2.337(10)	0.32(5)	1.23(10)	1.22(11)	0.95(9)
32	2.361(4)	2.347(5)	2.355(7)	2.350(10)	0.46(48)	1.41(27)	1.02(18)	1.07(17)
70	2.353(4)	2.352(6)	2.350(6)	2.352(11)	0.64(7)	1.30(23)	0.95(11)*	1.02(4)
100	2.360(3)	2.359(5)	2.359(9)	2.332(10)	0.63(3)*	1.05(7)*	1.01(5)	1.00(3)
130	2.360(4)	2.351(5)	2.362(8)	2.331(10)	0.69(3)*	1.07(9)	0.95(5)	1.08(3)
200	2.363(4)	2.357(6)	2.334(6)	2.344(14)	0.73(5)*	1.02(5)	1.07(4)	1.09(3)
400	2.356(3)	2.358(6)	2.359(8)	2.349(8)	0.92(5)*	0.96(5)	0.99(4)	1.06(3)
1000	2.351(4)	2.354(4)	2.351(10)	2.339(11)	0.94(6)*	0.87(8)*	1.01(3)	1.09(3)
10000	2.365(4)	2.352(5)	2.351(6)	2.341(13)	0.87(8)*	0.94(6)	1.02(4)	0.93(8)
∞	2.354(4)	2.360(6)	2.356(8)	2.334(11)	1.00(7)*	1.01(8)	1.05(3)	1.01(4)

Table 5: Same as in Table 4, except for variable field renormalization ξ and using fixed amount of noise, $a_w = 100$.

	λ_1				λ_2			
ξ	$k=1$	$k=2$	$k=3$	$k=4$	$k=1$	$k=2$	$k=3$	$k=4$
0.84	2.823(4)	2.831(9)	2.813(11)	2.790(10)	0.62(5)*	1.09(4)*	1.10(12)	1.12(4)
0.88	2.578(3)	2.581(5)	2.582(6)	2.567(11)	0.76(12)	0.99(8)	1.09(7)	1.06(5)
0.90	2.467(4)	2.463(6)	2.463(9)	2.426(13)	0.72(9)	1.06(11)	1.08(6)	1.13(5)
0.92	2.360(3)	2.359(6)	2.359(9)	2.332(10)	0.63(3)*	1.07(5)*)	1.01(5)	1.00(3)
0.94	2.169(3)	2.179(6)	2.164(6)	2.162(12)	0.62(11)*	1.16(8)	1.00(8)	0.94(4)
0.96	2.169(3)	2.179(6)	2.164(6)	2.162(12)	0.53(4)*	1.21(30)	1.00(6)	0.94(3)
1.00	1.993(3)	1.996(5)	1.986(7)	1.990(8)	0.58(3)*	0.91(9)	0.83(6)*	0.87(4)

Additional evidence for a fixed point structure is provided by the flow of the operators, Eq. (13), as the field blocking is iterated. This is demonstrated in Figure 6 for the expectation value of the operator $\mathcal{O}_1 = \langle \phi_i \square \phi_i \rangle$, both for $c_M = 1$ and 10. Notice that in order to eliminate undue influence of geometric finite-size effects, we only compare operators measured at the *same* blocked lattice volume, $N^{(k)} = 250$, but which corresponding to different amount of node decimation. For both models, the value of the operator changes substantially in the first blocking iteration; this indicates that bare model is relatively far away from the critical fixed point This effect is more pronounced for the $c_M = 10$ model, as discussed earlier. However, already after the second blocking of the fields, the operators appear to have converged to their fixed point values.

5 Discussion

Although there exists no analytic RG calculation for dynamical lattices, using the results of matrix model calculations one can nevertheless predict the appropriate
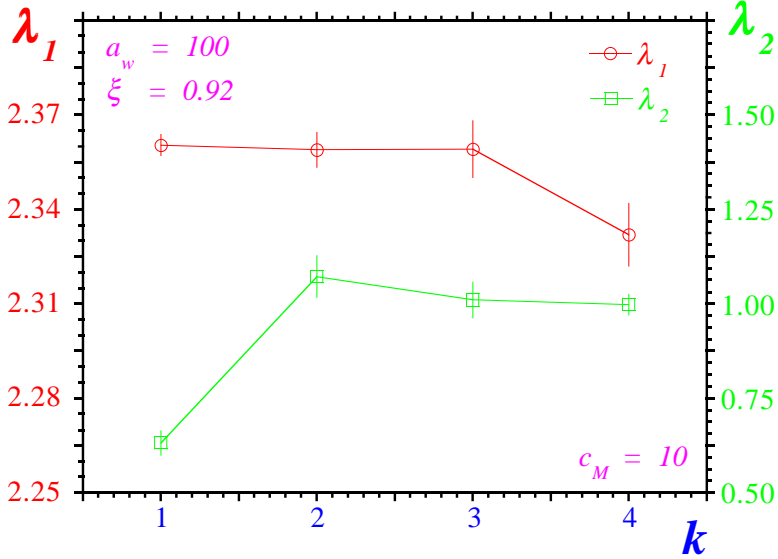
Figure 5: The two leading eigenvalues of the stability matrix for ten scalar fields ($c_M = 10$), using $a_w = 100$ and $\xi = 0.92$, *versus* the number of RG iterations k.

value of ξ, the field renormalization constant, for the case $c_M = 1$. Additionally, simple dimensional arguments yield an estimate of some of the eigenvalues of the stability matrix.

First lets look at the origin of the length dimension in the lattice fields. On the bare lattice we simulate a system with fields governed by the continuum action (let us take the internal dimension d to be arbitrary for the moment),

$$S_{\text{cont}} = \int \mathrm{d}^d x \sqrt{g} \, (\partial \phi_{\text{cont}}(x))^2 . \tag{17}$$

If we scatter points separated by a distance h throughout the manifold, we can approximate this action by

$$S_{\text{cont}} \approx \sum_{<i,j>} \frac{1}{h^2} \, (\phi_{\text{cont}}(x_i) - \phi_{\text{cont}}(x_j))^2 \, h^d. \tag{18}$$

To write this in terms of lattice fields, as we did in Eq. (2), requires

$$\phi_{\text{cont}} = \phi_{\text{lat}} h^{\frac{2-d}{2}}. \tag{19}$$

The continuum field, ϕ_{cont}, has length dimension $\beta = -\eta/2$ defined by the scaling of the geodesic two-point function,

$$\langle \phi_{\text{cont}}(x_i) \, \phi_{\text{cont}}(x_j) \rangle \sim r_{ij}^{-\eta}. \tag{20}$$

This implies that a change of the length scale of problem, $h \to sh$, should induce a change of scale of the (continuum) fields:

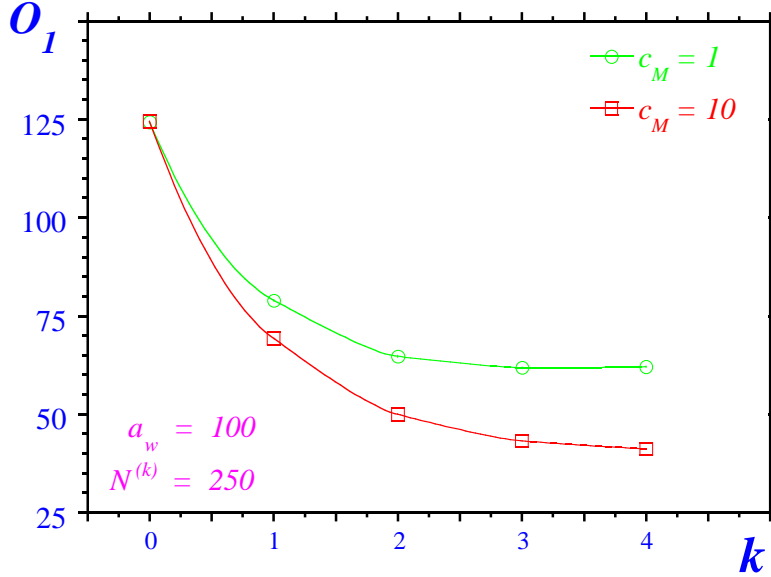$$\phi_{\text{cont}} \to \phi_{\text{cont}} s^{-\beta}. \tag{21}$$

13

Figure 6: The "flow" of the (normalized) operator $\mathcal{O}_1 = \langle\phi_i\Box\phi_i\rangle$ for both one and ten scalar fields. All the measurements are done on triangulations of volume 250, generated by different amount k of node decimation from bare lattices of volume $2^k 250$. The fields are blocked using $a_w = 100$, and $\xi = 1.00$ and 0.92 for $c = 1$ and 10 respectively.

For this to occur, the lattice fields must re-scale under such a change like

$$\phi_{\text{lat}} \rightarrow \phi_{\text{lat}} s^{\frac{d-2}{2}-\beta}. \tag{22}$$

In our lattice simulation we do not have direct access to the length scale, but we do have access to the volume scale. So on a lattice with fractal dimension d_H, a volume rescaling of $b = s^{d_H}$ requires the fields be rescaled like

$$\phi_{\text{lat}} \rightarrow \phi_{\text{lat}} b^{\frac{d-2-2\beta}{2d_H}}, \tag{23}$$

The implication then, is that in $d = 2$ the field renormalization constant

$$\xi = b^{-\frac{\beta}{d_H}}, \tag{24}$$

This is a generalization of the field renormalization constant given in Ref. [14].

Consider first the case $c_M = 1$. If we assume the action to be dimensionless, then we can count dimensions to show that the undressed length dimension for a Gaussian field in a flat two-dimensional space is zero:

$$S = \int d^2x (\partial\phi)^2 \implies \beta_0 = 0. \tag{25}$$

In the presence of quantum gravity, however, the field will in general develop an anomalous length dimension. For $c_M \leq 1$ we can use the well known KPZ [1] scaling relations:

$$\beta - \frac{\beta(1-\beta)}{1-\gamma_s} = \beta_0, \tag{26}$$

14

with

$$\gamma_s \;=\; \frac{1}{12}\left(c_M - 1 - \sqrt{(25 - c_M)(1 - c_M)}\right), \tag{27}$$

to find β, the dressed field dimension. So for $c_M = 1$,

$$\beta \;=\; \beta_0 \;=\; 0, \tag{28}$$

implying $\xi = 1$. For $c_M = 1$ our MCRG result of $\xi^* = 1.00(3)$ can be taken as an independent numerical determination of β consistent with Eq. (28). For $c_M = 10$, our result of $\xi^* = 0.92(4)$ would suggest that $\frac{\beta}{d_H} = 0.12(6)$.

Although meaningful analytical results are not available for $c_M > 1$, simple dimensional arguments showing consistency of our $c_M = 10$ results. Consider the operator $O_0 = \langle \sum_i \phi_i^2 \rangle$. From the analysis of the eigenvectors of the stability matrix this is essentially the operator corresponding to the leading eigenvalue. The simplest ansatz for its behavior under scaling follows from the scaling of the field in Eq. (23)

$$O_0 \;\to\; b^{-\frac{2\beta}{d_H}-1} O_0 \,.$$

The corresponding coupling constant g_{O_0} in a dimensionless action should re-scale inversely, like

$$g_{O_0} \;\to\; b^{1+\frac{2\beta}{d_H}} g_{O_0}, \tag{29}$$

suggesting that the leading relevant eigenvalue should be

$$\lambda_{O_0} \;=\; b^{1+\frac{2\beta}{d_H}}. \tag{30}$$

The extra factor of b is due to the change of the sum over N nodes to a sum over $N' = N/b$ nodes.

We note that substituting $\beta/d_H = 0$, for $c_M = 1$, and $\beta/d_H = 0.12$, for $c_M = 10$, gives $\lambda_{O_0} = 1.98(10)$ and $\lambda_{O_0} = 2.36(20)$, respectively. This is remarkably consistent with the leading eigenvalues we obtained for both cases.

The remaining check that we can institute is that the critical exponents extracted from the eigenvalues of the stability matrix are consistent with those obtained through finite-size scaling analysis. Simple arguments show that if an operator O at criticality scales like

$$\langle O \rangle \;\sim\; N^\mu \tag{31}$$

on lattices of volume N then there should be a leading eigenvalue

$$\lambda_1 \;=\; b^\mu. \tag{32}$$

Consider the leading operator O_0, again for $c_M = 10$. Its finite-size scaling is shown in Figure 7 and yields an exponent $\mu = 1.25(1)$. This is consistent with the leading eigenvalue $\lambda_1 = 2.36(20)$ extracted from the stability matrix (Figure 4.2).
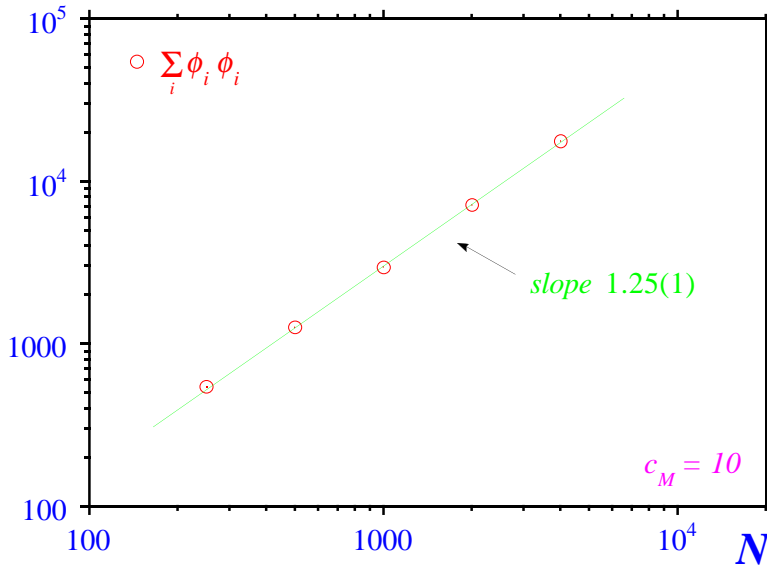
15

Figure 7: The volume scaling of the operator $\mathcal{O}_0 = \langle \sum_i \phi_i \phi_i \rangle$ measured on bare triangulations with $c_M = 10$. The straight line is a fit $\langle \sum_i \phi_i \phi_i \rangle \sim V^{1.25(1)}$.

6   Conclusions

We have successfully extended the renormalization group scheme for dynamical triangulations based on node decimation to the case of continuous scalar fields coupled to two-dimensional gravity. Results for the wave function renormalization constant ξ and hence $\frac{\eta}{d_H}$ together with the leading eigenvalue of the stability matrix are obtained for $c_M = 1$ and $c_M = 10$ which are consistent with theoretical expectations.

References

[1] F. David, *Mod. Phys. Lett. B* **186** (1987) 379;
J. Distler and H. Kawai, *Nucl. Phys. B* **321** (1989) 509;
V.G Knizhnik, A.M. Polyakov and A. Zamolodchikov, *Mod. Phys. Lett. A* **3** (1988) 819.

[2] G. Thorleifsson and S.M. Catterall, *Nucl. Phys. B* **461** (1996) 350.

[3] R.M. Neal, *Suppressing Random Walks in Markov Chain Monte Carlo Using Ordered Overrelaxation*, Technical report No. 9508, Dept. of Statistics, University of Toronto (`bayes-an/9506004`).

[4] I. Horváth and A.D. Kennedy, *Nucl. Phys. B* **510** (1998) 367.

[5] C.B. Lang, *Nucl. Phys. B* **265** (1986) 630.

[6] T.L. Bell and K.G. Wilson, *Phys. Rev. B* **11** (1975) 3431.

[7] S. Catterall, G. Thorleifsson, M. Bowick and V. John, *Phys. Lett. B* **354** (1995) 58.

[8] J. Ambjørn, J. Jurkiewicz and Y. Watabiki, *Nucl. Phys. B* **454** (1995) 313.

[9] J. Ambj orn and K.N. Anagnostopoulos, *Nucl. Phys. B* **497** (1997) 445.

[10] S. Jain and S.D. Mathur, *Phys. Lett. B* **286** (1992) 239.

[11] J. Ambjørn, S. Jain, and G. Thorleifsson, *Phys. Lett. B* **307** (1993) 34; J. Ambjørn, and G. Thorleifsson, *Phys. Lett. B* **323** (1994) 7.

[12] F. David, *Simplicial Quantum Gravity and Random Lattices*, (`hep-th/9303127`), Lectures given at Les Houches Summer School on Gravitation and Quantization, Session LVII, Les Houches, France, 1992; J. Ambjørn, *Quantization of Geometry*, (`hep-th/9411179`), Lectures given at Les Houches Summer School on Fluctuating Geometries and Statistical Mechanics, Session LXII, Les Houches, France 1994; P. Di Francesco, P. Ginzparg and J. Zinn-Justin, *Phys. Rep.* **254** (1995) 1.

[13] A. Bennett, *Nucl. Phys. B* **300** (1988) 253.

[14] T.L. Bell and K.G. Wilson, *Phys. Rev. B* **10** (1974) 3935.